NADPH oxidase is an O_2 sensor in airway chemoreceptors: Evidence from K^+ current modulation in wild-type and oxidase-deficient mice

Xiao Wen Fu*, Dashou Wang*, Colin A. Nurse†, Mary C. Dinauer‡, and Ernest Cutz*§

*Division of Pathology, Department of Pediatric Laboratory Medicine, The Research Institute, The Hospital for Sick Children and University of Toronto, 555 University Avenue, Toronto, ON M5G 1X8, Canada; †Department of Biology, McMaster University, Hamilton, ON L8S 4K1, Canada; and ‡Department of Medical and Molecular Genetics, Indiana University School of Medicine, Indianapolis, IN 46202

Communicated by Ewald R. Weibel, University of Bern, Herrenschwanden, Switzerland, February 9, 2000 (received for review November 30, 1999)

Pulmonary neuroepithelial bodies (NEBs) are presumed airway chemoreceptors that express the putative O_2 sensor protein NADPH oxidase and O_2-sensitive K^+ channels $K^+(O_2)$. Although there is a consensus that redox modulation of $K^+(O_2)$ may be a common O_2-sensing mechanism, the identity of the O_2 sensor and related coupling pathways are still controversial. To test whether NADPH oxidase is the O_2 sensor in NEB cells, we performed patch-clamp experiments on intact NEBs identified by neutral red staining in fresh lung slices from wild-type (WT) and oxidase-deficient (OD) mice. In OD mice, cytochrome b_{558} and oxidase function was disrupted in the $gp91^{phox}$ subunit coding region by insertion of a neomycin phosphotransferase (neo) gene. Expression in NEB cells of neo mRNA, a marker for nonfunctional $gp91^{phox}$, was confirmed by nonisotopic *in situ* hybridization. In WT cells, hypoxia (pO_2 = 15–20 mmHg; 1 mmHg = 133 Pa) caused a reversible inhibition (≈46%) of both Ca^{2+}-independent and Ca^{2+}-dependent K^+ currents. In contrast, hypoxia had no effect on K^+ current in OD cells, even though both K^+ current components were expressed. Diphenylene iodonium (1 μM), an inhibitor of the oxidase, reduced K^+ current by ≈30% in WT cells but had no effect in OD cells. Hydrogen peroxide (H_2O_2; 0.25 mM), a reactive oxygen species generated by functional NADPH oxidase, augmented K^+ current by >30% in both WT and OD cells; further, in WT cells, H_2O_2 restored K^+ current amplitude in the presence of diphenylene iodonium. We conclude that NADPH oxidase acts as the O_2 sensor in pulmonary airway chemoreceptors.

The neuroepithelial bodies (NEBs) are specialized pulmonary structures composed of clusters of innervated amine- and peptide-containing cells, widely distributed within airway mucosa of human and animal lungs (1–3). In most species, NEBs are located preferentially at or near airway bifurcation, a site ideally suited for sensing changes in airway gas concentration (4). Based on these anatomical features and experimental studies showing release of amine (serotonin) from NEB cells after exposure to acute hypoxia *in vivo* (5) or *in vitro* (6), it was suggested that NEBs may represent hypoxia-sensitive airway chemoreceptors. It has also been proposed that NEBs may be functionally analogous to glomus or type 1 cells of the carotid body, well defined arterial chemoreceptors (7). The role of NEB cells as airway O_2 sensors was strengthened recently by the demonstration that these cells transduce a hypoxic stimulus via a mechanism similar to that of carotid body glomus cells (8). The electrophysiological properties of cultured and intact NEB cells, including characterization of the O_2-sensitive K^+ current, have been elucidated further by whole-cell patch-clamp recording in fetal rabbit lung cultures (9) and in thin slices of neonatal rabbit lung (10), respectively.

The precise molecular mechanisms of O_2 sensing have not been defined fully, and some aspects remain controversial. According to the ''membrane model'' originally proposed for carotid body glomus cells (11, 12), the regulation of K^+ channels by hypoxia is indirect and is mediated through a membrane-bound O_2-sensing enzyme complex, such as NADPH oxidase, found in phagocytic cells (13–15). In this model, hypoxia affects oxidase function via decrease in substrate (O_2) availability, resulting in reduced production of O_2-reactive intermediates including H_2O_2 and redox modulation of K^+ channel activity (16). The downstream effects of K^+ channel closure by hypoxia include membrane depolarization, leading to the opening of voltage-activated Ca^{2+} channels, increase in intracellular Ca^{2+}, and neurotransmitter release.

Evidence for a potential role of NADPH oxidase as an O_2-sensor enzyme complex in carotid body glomus cells and other O_2-sensing cells has been reviewed by Acker and Xue (15). In pulmonary NEBs, a multicomponent NADPH oxidase similar to that found in phagocytic cells has been identified by using immunohistochemical and molecular techniques (8, 9, 17). In particular, mRNA transcripts for type *b* cytochrome ($gp9^{phox}$ and $p22^{phox}$) and corresponding proteins have been localized in NEBs of rabbit fetal and human neonatal lungs (9, 17). The cytosolic components $p47^{phox}$, $p67^{phox}$, and rac 2 have also been identified in cultures of rabbit fetal NEBs by using immunohistochemical methods (17). Furthermore, a functional oxidase has been identified in cultures of rabbit fetal NEBs by using dihydrorhodamine 123 as a probe for H_2O_2 generation (9). In this assay, diphenylene iodonium (DPI), an inhibitor of the flavoprotein component of the oxidase, caused decrease in H_2O_2 production, whereas incubation with phorbol ester, acting via phosphorylation of $p47^{phox}$ component, caused up to a 3-fold increase in H_2O_2 production (9).

The availability of a NADPH oxidase-deficient (OD) mouse model, lacking functional $gp91^{phox}$ subunit of the oxidase (18), provides a unique opportunity to test the hypothesis regarding the role of the oxidase in O_2 sensing. In this study, we examined the lungs of OD mice for the expression of defective $gp91^{phox}$ gene in NEB cells by using nonisotopic *in situ* hybridization (NISH). The electrophysiology of NEBs in both wild-type (WT) and OD mice was studied by using fresh lung slice preparation and whole-cell recording. During the course of these studies, a report based on the use of an identical OD mouse model was published (19), indicating that NADPH oxidase was not an O_2 sensor in pulmonary artery smooth muscle cells. Our results on pulmonary NEB cells led to the opposite conclusion for airway chemoreceptors, i.e., NADPH oxidase is an airway O_2 sensor.

Methods

Animal Models. The OD mice ($gp91^{phox}$ knockout; X-linked chronic granulomatous disease) were obtained from M.C.D.

Abbreviations: NEB, neuroepithelial body; WT, wild type; OD, oxidase-deficient; DPI, diphenylene iodonium; CGRP, calcitonin gene-related peptide; NISH, nonisotopic *in situ* hybridization; TEA, tetraethylammonium; *I–V*, current–voltage; PASMC, pulmonary artery smooth muscle cells.

§To whom reprint requests should be addressed. E-mail: ernest.cutz@sickkids.on.ca.

The publication costs of this article were defrayed in part by page charge payment. This article must therefore be hereby marked "*advertisement*" in accordance with 18 U.S.C. §1734 solely to indicate this fact.

(18). Based on the derivation of the original founder mice with X-linked chronic granulomatous disease, we used the black C57BL/6J mice (The Jackson Laboratory) as a control group (WT). For all studies, we used newborn animals (1–7 days old) of both sexes. The mice were euthanized by an i.p. injection of Euthanyl (pentobarbital sodium; 100 mg·kg^{-1}).

Immunohistochemistry. For microscopic studies, lungs from WT and OD mice were fixed in 10% (vol/vol) neutral buffered formalin and embedded in paraffin. For identification of NEBs in lung sections, we used an immunohistochemical method for localization of the calcitonin gene-related peptide (CGRP), a marker of NEB in rodent lungs (20).

The Preparation of cRNA Probe for Localization of Nonfunctional gp91^{phox} Gene. The NADPH OD mouse model with a null allele for gp91^{phox} was generated by insertion of the neomycin phosphotransferase gene into the mid portion of exon 3 in the gp91^{phox} gene (18). To generate a probe for localization of nonfunctional gp91^{phox} gene, we used a neomycin phosphotransferase cDNA synthesized by PCR. We used pCI-neo vector (Promega) as the template and selected the following two oligomers: ACAAGATGGATTGCACGC (representing 2,473–2,479 bp of pCI-neo) and CCATCGTGATGGCAGGTT (representing 3,301–3,318 bp of pCI-neo).

The PCR was carried out at 95°C for 1 min and 60°C for 1 min for 30 cycles. A 850-bp fragment was amplified and subcloned subsequently to pCR2.1 vector (neo clone). The neo clone was linearized by restriction enzyme *Hin*dIII, and we used T7 RNA polymerase to synthesize neo-cRNA probe in the presence of digoxigenin-11-UTP.

***In Situ* Hybridization.** For identification of defective gp91^{phox} gene in NEB cells, we used NISH. The protocol for NISH with digoxigenin-labeled neo-cRNA probe was similar to the one described in ref. 21. Detection was achieved with application of the Dig Nucleic Acid Detection Kit (Roche Molecular Biochemicals). After color development, the slides were mounted in a routine fashion. In most experiments, lung sections were immunostained first for CGRP to identify NEBs, followed by NISH.

Electrophysiology. Fresh lung tissue slices were prepared as described (10). The perfusing Krebs solution had the following composition (in mM): 130 NaCl, 3 KCl, 2.5 $CaCl_2$, 1 MgCl, 10 $NaHCO_3$, 10 Hepes, and 10 glucose (pH ≈7.35–7.4). In some experiments, $CaCl_2$ was replaced by 1.5 mM $CoCl_2$ to eliminate calcium entry. To identify NEB cells in fresh lung tissue, the slices were incubated with vital dye neutral red (0.02 mg/ml^{-1}) for 1 h at 37°C (9).

Whole-cell currents in NEB cells were recorded by using protocols and instrumentation as described (10, 22). The recording electrodes (resistance of 3–5 MΩ) contained solution with the following composition (in mM): 130 KCl or 100 K-gluconate, 30 KCl, 1 $MgCl_2$, 4 Mg-ATP, 5 EGTA, and 10 Hepes (11). The pH of the internal solution was adjusted to 7.25 with KOH. Hypoxic solutions were prepared as described (10). The pO_2 of control solution was 145–155 mmHg (1 mmHg = 133 Pa), compared with 15–20 mmHg for the hypoxic solution.

The resting membrane potential was measured in current-clamp mode soon after membrane rupture in cell-attached configuration. The passive properties, i.e., input resistance (R_m), capacitance (C_m), and time constant ($\tau_m = R_m \times C_m$), were calculated as described (10). All values are given as means ± SEM. Statistical analysis was performed by using the paired and unpaired Student's t test. Differences were considered statistically significant when $P < 0.05$.

The drugs tetraethylammonium (TEA), 4-aminopyridine, DPI, and hydrogen peroxide (H_2O_2) were obtained from Sigma. All experiments were carried out with approval and in accordance with Institutional Guidelines for Animal Care.

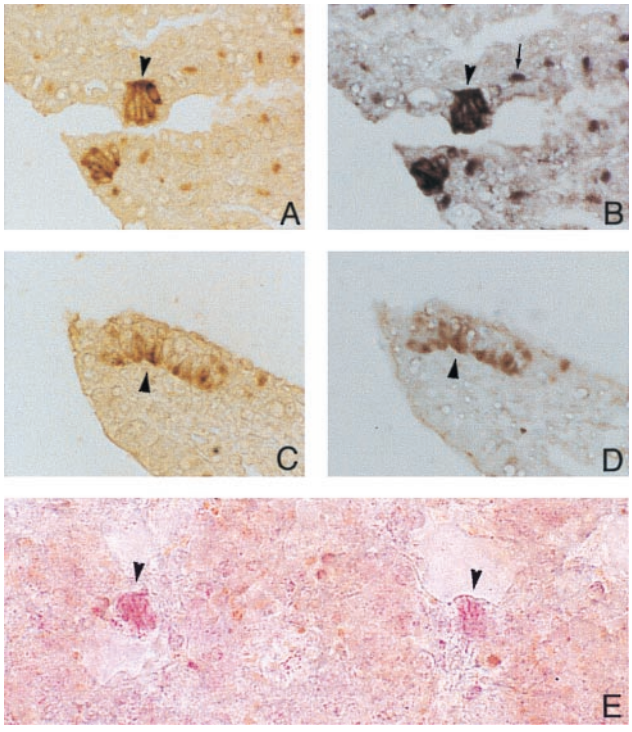

Fig. 1. Identification of NEBs in lungs of OD and WT mice. (*A*) CGRP-positive NEB cells (brown color; arrowhead) in OD mouse. Light brown staining of macrophages is possibly due to increased endogenous peroxidase in OD mice, because no such staining was seen in WT mice. (*B*) Same area shown in *A* after immunostaining followed by NISH with neo-cRNA probe; the specific signal (dark purple color) shows reactivity in the same NEB cells (arrowhead) stained in *A*, indicating expression of nonfunctional NADPH oxidase gene. Macrophages in peribronchial tissue show positive reaction for neo (arrow). (*C*) CGRP-positive NEB cells (brown color; arrowhead) in WT mouse. (*D*) Same area shown in *C* after immunostaining followed by NISH with neo-cRNA probe; there is no positive signal in NEB cells (arrowhead) or macrophages. (*E*) Two NEBs stained by neutral red (arrowheads) in fresh lung slice from WT mouse. (Magnifications: *A–D*, ×400; *E*, ×250).

Results

Identification of NEBs and Localization of Nonfunctional gp91^{phox} Gene in the Lung. The overall lung histology in neonatal OD mice was similar to that in WT animals. In sections immunostained for CGRP, clusters of positive cells with features of NEBs were identified in airways of both OD and WT mice (Fig. 1 *A* and *C*, respectively). The overall number, distribution, and size of NEBs were comparable in OD and WT mice. In samples processed for NISH, the lung sections incubated with antisense probe for neomycin phosphotransferase (neo) mRNA showed strong positive signal in the cytoplasm of NEB cells of OD mice (Fig. 1*B*) but not of WT mice (Fig. 1*D*). In addition to NEB cells, macrophages in alveolar septae also expressed the neo in OD mice but not in WT mice (Fig. 1 *B* and *D*).

Passive Membrane Properties of NEB cells in WT and OD mice. In fresh lung slices from both WT and OD mice incubated with neutral red dye, NEB cells appeared as reddish-pink cell clusters within the airway epithelium (Fig. 1*E*). Whole-cell patch-clamp recordings were obtained from NEB cells of WT mice ($n = 52$) and OD mice ($n = 65$). The mean resting potential was −50.1 ± 0.9 mV ($n = 12$) in NEB cells from WT mice versus −51.9 ± 1.9 mV ($n =$

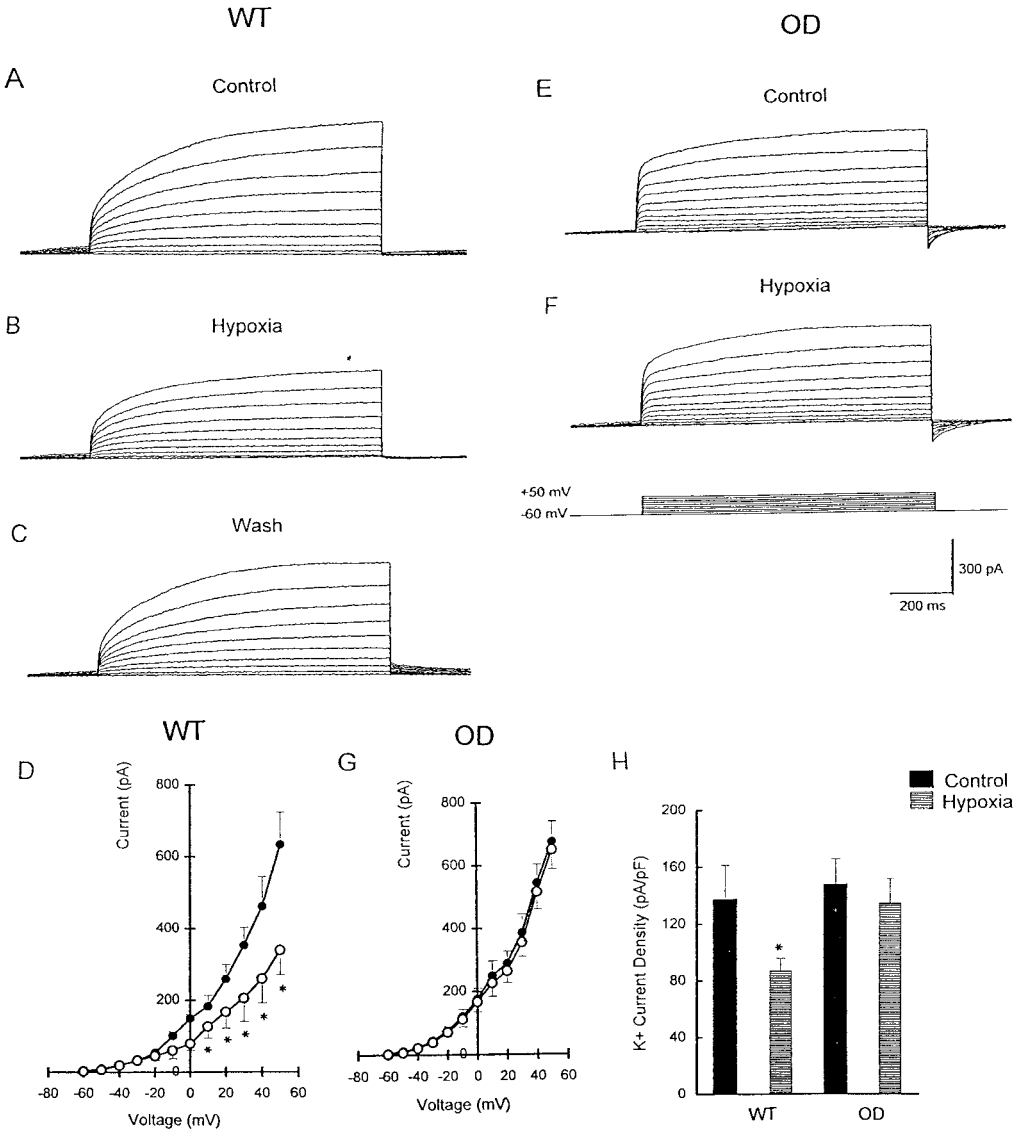

Fig. 2. Effect of hypoxia on K^+ current in NEB cells of WT versus OD mice. (*A*) Outward K^+ current in WT cells evoked by depolarizing steps from −60 mV to +50 mV in control Krebs solution. (*B*) Outward current as described for *A* was inhibited by hypoxia, and the effect was reversible (*C*). (*D*) Current–voltage (*I–V*) relationship for WT cells in control (●) and hypoxic solution (○). Holding potential was −60 mV (*, $P < 0.05$; $n = 9$). (*E*) K^+ current in OD cells evoked by depolarizing steps from −60 mV to +50 mV in control solution. (*F*) Hypoxic solution failed to reduce K^+ currents in OD cells. (*G*) *I–V* relationship was similar for OD cells ($n = 12$) in control (●) and hypoxic solution (○). (*H*) Comparison of K^+ current density in WT and OD cells under control (black bars) and hypoxic (hatched bars) conditions. Current density estimated by dividing peak current (+50-mV test potential) by input capacitance. K^+ current density was decreased significantly (relative to control) during hypoxia in WT cells ($n = 8$; *, $P < 0.05$); in contrast, hypoxia had no effect on K^+ current density in OD cells ($n = 8$).

15) in those from OD mice. The mean input resistance and capacitance was 1.09 ± 0.07 GΩ ($n = 19$) and 2.64 ± 0.06 pF ($n = 38$), respectively, in WT mice versus 1.16 ± 0.08 GΩ ($n = 19$) and 2.54 ± 0.04 pF ($n = 29$), respectively, in OD mice. The mean membrane time constant was 2.74 ± 0.19 ms ($n = 19$) in WT mice and 3.0 ± 0.22 ms ($n = 19$) in OD mice. There were no significant differences in resting membrane potential, input resistance, capacitance, and membrane time constant between NEB cells of WT and OD mice ($P > 0.05$).

Effects of Hypoxia on K^+ Currents in NEB Cells of WT and OD Mice. Depolarizing steps from a holding potential of −60 mV to +50 mV evoked outward K^+ currents in the majority (90%) of NEB cells from both WT and OD mice (Fig. 2 *A* and *E*). Exposure to hypoxia caused a rapid and reversible suppression of K^+ current by ≈46% in WT cells (Fig. 2 *A–C*), and the effect was significant at voltage steps >0 mV (Fig. 2*D*). After a return to normoxia, K^+ current amplitude recovered to a value not significantly different from that of the initial control (Fig. 2*C*). In contrast, hypoxia had no significant effect on K^+ current in NEB cells of OD mice at all test potentials (Fig. 2 *E–G*). Because WT and OD cells had different responses to hypoxia, it was of interest to compare current densities by dividing peak current by whole-cell capacitance. As shown in Fig. 2*H*, the mean K^+ current density in NEB cells of WT mice was significantly ($P < 0.05$) lower during hypoxia (87.0 ± 8.9 pA/pF; $n = 8$) relative to control normoxia (137 ± 24.3 pA/pF). In OD cells, although K^+ current density seemed slightly larger in control conditions, there was no statistically significant difference during hypoxia.

The outward K^+ current in NEB cells of both WT and OD

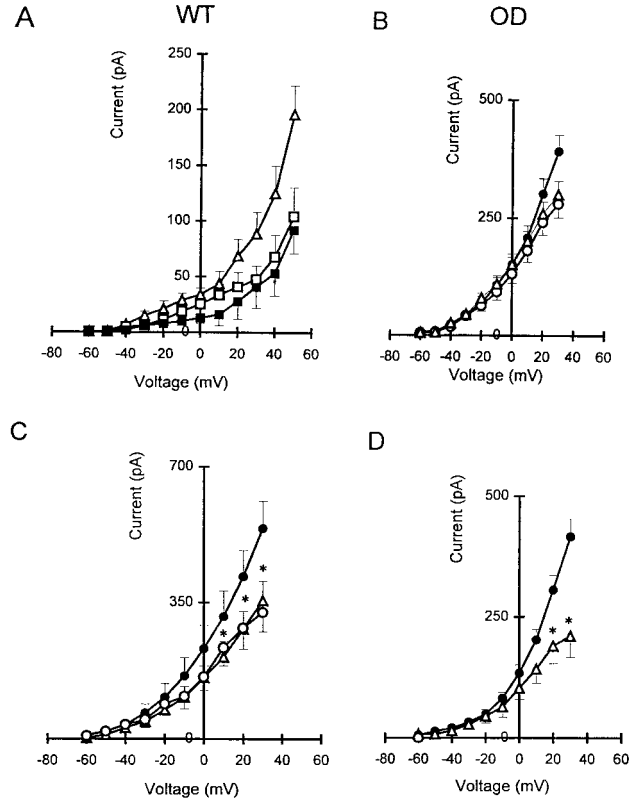

Fig. 3. Electrophysiological and pharmacological characterization of whole-cell K^+ current (I_K) in NEB cells of WT and OD mice. (*A*) *I–V* relationships obtained from the total hypoxia-sensitive K^+ current (△), hypoxia-sensitive $I_{K(V)}$ current (□), and hypoxia-sensitive $I_{K(Ca)}$ current (■) in NEB cells of WT mice. Data are shown as means ± SEM ($n = 4$). (*B*) In NEBs of OD mice, there was ≈29% reduction in K^+ current in the *I–V* relationship after perfusion of cells with Ca^{2+}-free solution (△) compared with cells in the control solution (●), but perfusion with Ca^{2+}-free solution plus hypoxia (○) had no effect. (*C*) *I–V* relationship for WT cells ($n = 10$) in control (●), during perfusion of 20 mM TEA (△; $n = 10$), and during perfusion of 20 mM TEA plus hypoxia (○; $n = 4$). (*D*) *I–V* relationship for OD cells ($n = 12$) in control (●) and after perfusion with 20 mM TEA (△; $n = 4$). *, $P < 0.05$.

mice consisted of two components, a Ca^{2+}-dependent K^+ current [$I_{k(Ca)}$] and a Ca^{2+}-insensitive, voltage-dependent K^+ current [$I_{K(V)}$] (Fig. 3*A*). Both components contributed to hypoxic sensitivity in WT cells exposed to hypoxia before and during perfusion of Ca^{2+}-free solution as reported for NEBs of neonatal rabbits (10).

The lack of O_2 sensitivity in mutant NEB cells described above is likely due to the loss of O_2 sensor protein function in OD mice. Alternatively, the hypoxia-sensitive K^+ channel subtypes may not be expressed in NEB cells of OD mice. This alternative seems unlikely, however, because both Ca^{2+}-dependent and Ca^{2+}-independent outward K^+ currents were present in OD cells. Perfusion of NEB cells ($n = 4$) from OD mice with Ca^{2+}-free solution resulted in K^+ current reduction by ≈29%, comparable to that of WT mice (Fig. 3*B*). Further, in the presence of Ca^{2+}-free solution, hypoxia again failed to reduce the residual K^+ current in NEB cells ($n = 4$) of OD mice (Fig. 3*B*), implying that a substantial Ca^{2+}-independent K^+ current [$I_{k(v)}$] was present but hypoxia insensitive. Additional pharmacological tests (see below) indicated that a near normal complement of K^+ channels was expressed in OD cells.

Effects of TEA and 4-Aminopyridine on K^+ Current in NEB Cells of WT and OD Mice. Pharmacology of the K^+ outward current in NEB cells of WT and OD mice was carried out by testing the effect of the K^+ channel blocker TEA (20 mM; Fig. 3 *C* and *D*). In WT cells, TEA reversibly suppressed K^+ current amplitude at voltages between +10 mV and +30 mV ($P < 0.05$; $n = 10$; Fig. 3*C*). Further, in the presence of TEA, hypoxia had no effect on the residual K^+ current (Fig. 3*C*). Current amplitudes at +30-mV test potential before and during application of 20 mM TEA were reduced by ≈34%. The K^+ current recorded in TEA plus hypoxia at +30-mV test potential was not significantly different from that recorded in TEA alone. These data indicate that the O_2-sensitive K^+ current in NEB cells of WT mice is also TEA sensitive, as reported recently for NEB cells of neonatal rabbit (10). The aminopyridine 4-aminopyridine (2 mM), a blocker of the delayed rectifier $I_{K(v)}$, also reduced K^+ current in WT cells (data not shown).

In NEB cells from OD mice, 20 mM TEA reversibly inhibited K^+ current evoked at more positive potentials, and the effect was significant between +20 mV and +30 mV (Fig. 3*D*). Current amplitude at +30-mV test potential before and during application of 20 mM TEA was 416.2 ± 37 pA and 209.9 ± 44.8 pA, respectively, corresponding to a reduction by ≈49%. K^+ current was reduced by 43.9 ± 6.8% ($P < 0.05$; $n = 4$) at +30-mV test potential in the presence of 2 mM 4-aminopyridine (not shown), suggesting that delayed rectifier $I_{K(v)}$ channels were expressed in OD cells. These data suggested that voltage-gated K^+ channels in NEB cells of OD mice have pharmacological characteristics similar to those of WT mice; however, the channels present in OD cells did not respond to hypoxia.

Effect of DPI and H_2O_2 on K^+ Current in NEBs of WT and OD Mice. The effects of DPI (1–5 μM), an inhibitor of NADPH oxidase (23), were tested on K^+ currents in NEB cells from WT and OD mice. Bath application of 1 μM DPI inhibited K^+ current evoked at more depolarized potentials in WT cells (Fig. 4 *A–C*). K^+ current amplitude at +50-mV test potential before and during DPI application was significantly suppressed ($P < 0.05$; $n = 6$). Consistent with the results from OD mice, hypoxia had no effect on WT cells when oxidase function was inhibited by 1 μM DPI (data not shown).

In contrast to the effects of DPI, 0.25 mM H_2O_2 augmented K^+ current by ≈34% at +50-mV test potential, and the effect was significant between +10 mV and +30 mV (Fig. 4*A*, triangles). Interestingly, the inhibitory action of 1 μM DPI on K^+ current was reversed, and the current was potentiated, when H_2O_2 was present simultaneously (Fig. 4 *B–D*). Whereas K^+ current was reduced 32.9 ± 1.3% ($P < 0.01$; $n = 4$; Fig. 4*C*) by 1 μM DPI, addition of H_2O_2 (0.25 mM) in the presence of DPI increased K^+ current by 37.8 ± 4.3% ($P < 0.05$; $n = 4$; Fig. 4 *C* and *D*). The effects of both DPI and H_2O_2 were reversible.

In NEB cells of OD mice, the effect of DPI on K^+ current depended on drug concentration. At low concentrations (1 μM), DPI had no significant effect on K^+ current evoked at depolarized potentials in OD cells (Fig. 4*F*). These results contrast with those from WT cells, where 1 μM DPI inhibited K^+ current (Fig. 4*A*). At higher concentrations (5 μM), however, DPI inhibited K^+ current in OD cells by ≈49% (Fig. 4*F*). The concentration–inhibition curve for DPI on K^+ current in OD cells shows significant ($P < 0.05$) reversible inhibition between 2 and 5 μM DPI; the IC_{50} value for this inhibition was 3.65 μM. These results indicate that at low concentrations (1 μM), DPI may block the O_2-sensitive K^+ current selectively in NEB cells of WT mice, presumably via its known inhibitory effect on NADPH oxidase function (23). However, at higher doses (e.g., 5 μM), the effects seem nonselective as previously suggested (24, 25). In OD cells, application of 0.25 mM H_2O_2 reversibly increased K^+ current by ≈31% (Fig. 4*H*).

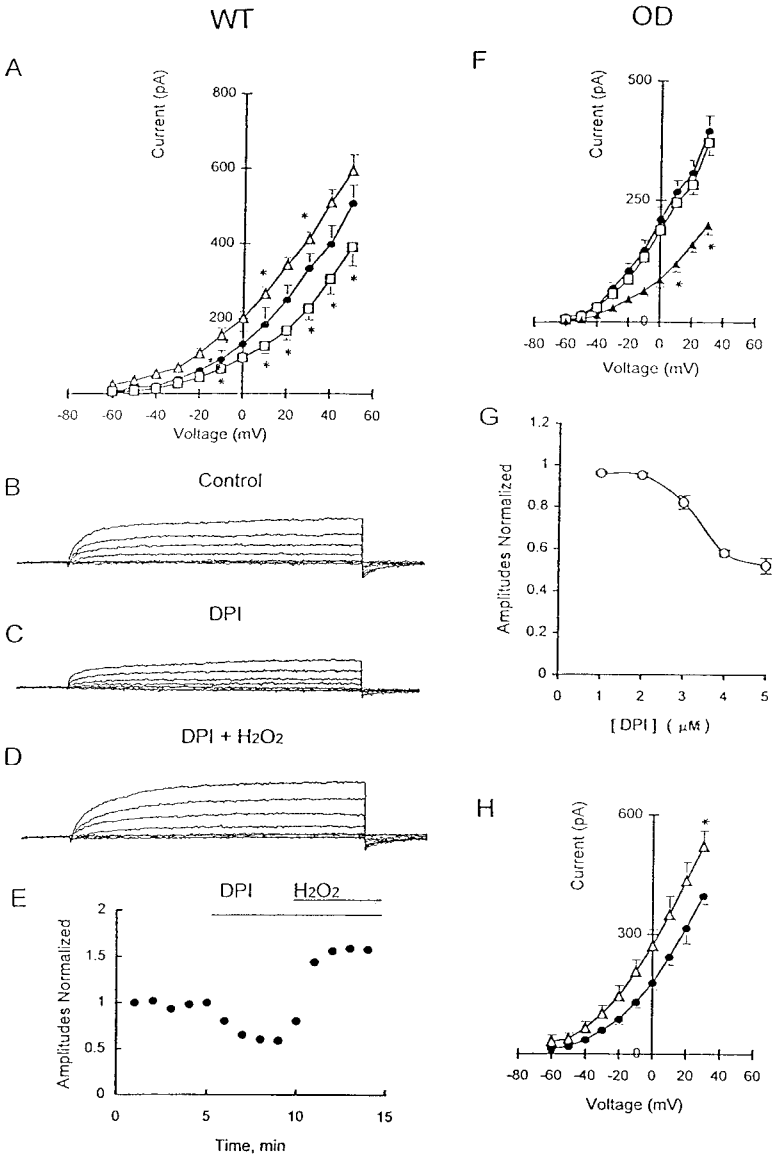

Fig. 4. Effects of DPI and H_2O_2 on the K^+ current in NEB cells of WT and OD mice. (*A*) *I–V* relationship for WT cells under control conditions (●; $n = 7$) or during perfusion with 1 μM DPI (□; $n = 6$) or with 0.25 mM H_2O_2 (△; $n = 4$). *, $P < 0.05$. Outward K^+ current evoked by depolarizing steps from −60 mV to +30 mV in control solution (*B*) was reduced during bath application of 1 μM DPI (C) and augmented ≈37% during combined exposure to 0.25 mM H_2O_2 and 1 μM DPI (*D*). (*E*) Time course of normalized K^+ current amplitude after application of DPI and DPI plus H_2O_2. All responses were normalized to peak current under control conditions (+30-mV test potential). (*F*) *I–V* relationship for OD cells under control conditions (●; $n = 9$) and after perfusing DPI at 1 μM (□; $n = 6$) and at 5 μM (▲; $n = 6$) DPI. *, $P < 0.05$. (*G*) Dose-response relationship for DPI; responses were normalized to the peak control current at +30-mV test potential. (*H*) *I–V* relationship for OD cells in control solution (●) and after perfusing 0.25 mM H_2O_2 (△). *, $P < 0.05$.

Discussion

In the present study, we used a transgenic approach to test the hypothesis that NADPH oxidase is an O_2 sensor in lungs of neonatal mice. During the neonatal period, the putative O_2 chemoreceptors or NEBs are most prominent and play a potential role in neonatal adaptation (26). Based on immunostaining for CGRP, the distribution and size of NEBs in lungs of mutant OD mice seemed comparable to those of WT controls. In OD mice, the X-linked gene for $gp91^{phox}$ has been displaced by insertion of a phosphoglycerol kinase (PGK) promoter-driven neomycin phosphotransferase gene in exon 3 (18). The expression of nonfunctional $gp91^{phox}$ gene in OD lungs was indicated by *in situ* hybridization with neo-cRNA probe as a marker. In theory, the PGK-neo gene should be "on" in all cells of OD mice. However, we observed high levels of expression of neo mRNA only in NEB cells and macrophages of the lung, suggesting that PGK-neo expression is silenced in cells that do not normally express $gp91^{phox}$. Our findings also suggest that the oxidase expressed in NEB cells may be genetically identical to the phagocyte oxidase, because at least one other candidate O_2-sensing protein, a $pg91^{phox}$ homolog mox-1, has been identified in nonphagocytic cells (27). Although high levels of mox-1 mRNA expression were found in colon, prostate, and aortic smooth muscle cells, extracts of human lung showed no expression. Initial studies on oxidase expression and function in OD mice have shown absence of $gp91^{phox}$ protein from phagocytic cells in both chimeric male and carrier female mice (18). Furthermore, superoxide formation was undetectable, indicat-

ing the absence of respiratory burst oxidase activity. Other studies that used the chemiluminescence assay to assess oxidase function have shown a marked reduction in the generation of active oxygen species in lung tissue of OD mice compared with that of WT controls (19). These data, together with our demonstration of defective pg91^{phox} gene expression, indicate that oxidase activity in NEB cells of OD mice is also nonfunctional.

Pharmacological analysis of voltage-activated currents indicated that NEB cells from WT and OD mice had a similar complement of voltage and Ca^{2+}-dependent K^+ channels. Because similar K^+ currents were expressed in WT and OD cells, the failure of hypoxia to suppress K^+ current in OD cells is most readily explained by lack of NADPH oxidase function. In support of this conclusion, 1 μM DPI, an inhibitor of the oxidase, inhibited K^+ current and particularly the O_2-sensitive component in NEB cells of WT mice but had no significant effect on K^+ current in OD cells. However, at higher concentrations, DPI (5 μM) inhibited K^+ current by $\approx$49% in NEB cells of both WT and OD mice, presumably because of a nonselective effect on ion channels (24, 25). In NEB cells of WT mice, external application of H_2O_2 augmented K^+ current, even in the continued presence of 1 μM DPI. This result is in contrast to a previous report in which application of H_2O_2 failed to restore K^+ current in pulmonary artery smooth muscle cells (PASMC) when 10 μM DPI was present (24). Although this discrepancy may be simply due to the different DPI concentrations used, our data suggest that, at low concentrations, DPI may still serve as a useful tool for selective inhibition of NADPH oxidase in O_2-sensing cells. In NEB cells, the inhibitory actions of DPI on K^+ currents seem to be mediated via inhibition of NADPH oxidase and H_2O_2 production. Indeed, external application of H_2O_2 increased K^+ currents in both WT and OD cells, suggesting that redox mechanisms for K^+ channel regulation were not impaired by the gp91^{phox} mutation. These findings provide strong evidence that the H_2O_2-generating system via NADPH oxidase plays an important role in hypoxic modulation of K^+ channels in pulmonary NEB cells and support the proposal for a close interaction between the oxidase and O_2-sensitive K^+ channels (9, 11, 15).

Our findings in pulmonary NEBs of OD mice are at variance with those recently reported on PASMC from the same mouse model by Archer *et al.* (19). These investigators reported that, in OD mice, K^+ current in PASMC was inhibited by hypoxia and that hypoxic pulmonary vasoconstriction in isolated lung preparation was maintained at levels comparable to those of WT animals (19). This study concluded that neither the multicomponent NADPH oxidase nor its low output variants are involved directly in O_2 sensing by PASMC. There are several possible explanations for the apparent discrepancies between our findings and those of Archer *et al.* (19). As pointed out by the latter investigators, NADPH oxidase may not be a "universal" O_2 sensor, and the particular one expressed in a given tissue may be modified appropriately for the level and range of local hypoxia and/or developmental stage.

The original "membrane model" of O_2 sensing envisaged three possibilities: (*i*) the ion channel itself is an O_2 sensor; (*ii*) the ion channel is modulated by an independent O_2 sensor via a diffusible cytoplasmic mediator; and (*iii*) the ion channel is associated closely with a membrane-bound O_2-sensing protein, such as NADPH oxidase, and the interaction occurs via a membrane-delimited pathway (11, 28). Evidence is accumulating in support of all three alternatives. For example, Chinese hamster ovary cells transfected with Shaker B cDNA have shown modulation of expressed K^+ channels by hypoxia in the absence of demonstrable NADPH oxidase in these cells (28). Other ion channels, such as the pore-forming α-subunit of human cardiac L-type Ca^{2+} channel expressed in HEK293 cells, show striking O_2 sensitivity (29). The recent findings of Archer *et al.* (19) in PASMC favor the second alternative with an independent cytosolic sensor (generated via the mitochondria) interacting with the K^+ channel. Our findings in pulmonary NEBs favor the third option in which there is close interaction between a membrane-bound oxidase and the K^+ channel. Such diversity and complexity of O_2-sensing mechanisms is not surprising given the vital role of O_2 in cell and organ function. Clearly the relative importance of different molecular mechanisms in O_2 sensing needs further investigation. The use of knockout mouse models, including OD mice, can provide mechanistic insight at the cellular, molecular, and whole-animal levels.

This work was supported by grants from Nicole Fealdman Sudden Infant Death Syndrome Research Fund (to E.C.) and by Medical Research Council of Canada Grant MT-12742 (to E.C. and C.N.). M.C.D. was supported by National Institutes of Health Grant HL 52565.

1. Lauweryns, J. M., Cokelaere, M. & Theunyck, P. (1972) *Z. Zellforsch. Mikrosk. Anat.* **135,** 569–592.
2. Sorokin, S. P. & Hoyt, R. F. (1989) in *Lung Cell Biology*, ed. Massaro, D. (Dekker, New York), pp. 199–344.
3. Cutz, E. (1997) in *Cellular and Molecular Biology of Airway Chemoreceptors*, ed. Cutz, E. (Landes Bioscience, Austin, TX), pp. 1–33.
4. Cho, T., Chan, W. & Cutz, E. (1989) *Cell Tissue Res.* **255,** 353–362.
5. Lauweryns, J. M., Cokelaere, M., Deleersnyder, M. & Liebens, M. (1977) *Cell Tissue Res.* **182,** 425–440.
6. Cutz, E., Spiers, V., Yeger, H., Newman, C., Wang, D. & Perrin, D. (1993) *Anat. Rec.* **236,** 41–52.
7. Gonzalez, C., Almaraz, L., Obeso, A. & Rigual, R. (1994) *Physiol. Rev.* **74,** 829–898.
8. Youngson, C., Nurse, C., Yeger, H. & Cutz, E. (1993) *Nature (London)* **365,** 153–155.
9. Wang, D., Youngson, C., Wong, V., Yeger, H., Dinauer, M., Vega-Saenz de Miera, E., Rudy, B. & Cutz, E. (1996) *Proc. Natl. Acad. Sci. USA* **93,** 13182–13187.
10. Fu, X. W., Nurse, C. A., Wang, Y. T. & Cutz, E. (1999) *J. Physiol. (London)* **514,** 139–150.
11. Lopez-Barneo, J., Alberto, R., Benot, A. R. & Urena, J. (1993) *News Physiol. Sci.* **3,** 191–195.
12. Lopez-Barneo, J. (1996) *Trends Neurosci.* **19,** 435–440.
13. Babior, B. M. (1992) *Adv. Enzymol Relat. Areas Mol. Biol.* **65,** 49–95.
14. Cross, A. R., Henderson, L., Jones, O. T. G., Delpiano, M. A., Hescheler, J. & Acker, H. (1990) *Biochem. J.* **272,** 743–747.
15. Acker, H. & Xue, D. (1995) *News Physiol. Sci.* **10,** 211–216.
16. Ruppersberg, J., Stocker, M., Pongs, O., Heinemann, S., Frank, R. & Koenen, M. (1991) *Nature (London)* **352,** 711–714.
17. Youngson, C., Nurse, C., Yeger, H., Curnutte, J. T., Vollmer, C., Wong, V. & Cutz, E. (1997) *Microsc. Res. Tech.* **37,** 101–106.
18. Pollock, J. D., Williams, D. A., Gifford, M. A. C., Li, L. L., Du, X., Fisherman, J., Orkin, S. H., Doerschuk, C. M. & Dinauer, M. C. (1995) *Nat. Genet.* **9,** 202–209.
19. Archer, S. L., Reeve, H. L., Michelakis, E., Puttagunta, L., Waite, R., Nelson, D. P., Dinauer, M. C. & Weir, E. K. (1999) *Proc. Natl. Acad. Sci. USA* **96,** 7944–7949.
20. Ijsselstijn, H., Hung, N., de Jongste, J. C., Tibboel, D. & Cutz, E. (1998) *Am. J. Respir. Cell Mol. Biol.* **19,** 278–285.
21. Wang, D. & Cutz, E. (1994) *Lab. Invest.* **70,** 775–780.
22. Hamill, O. P., Marty, A., Neher, E., Sakmann, B. & Sigworth, F. J. (1981) *Pflügers Arch.* **391,** 85–100.
23. Cross, A. R. & Jones, O. T. (1986) *Biochem. J.* **237,** 111–116.
24. Weir, E. K., Wyatt, C. H., Reeve, H. L., Huang, J., Archer, S. L. & Peers, C. (1994) *J. Appl. Physiol.* **76,** 2611–2615.
25. Wyatt, C. N., Weir, E. K. & Peers, C. (1994) *Neurosci. Lett.* **172,** 63–66.
26. Cutz, E., Gillan, J. E. & Bryan, A. C. (1985) *Pediatr. Pulmonol.* **1**, Suppl., S21–S29.
27. Suh, Y. A., Arnold, R. S., Lessegue, B., Shi, J., Xu, X., Sorescu, D., Chung, A. B., Griendling, K. K. & Lambeth, J. D. (1999) *Nature (London)* **401,** 79–82.
28. Lopez-Barneo, J., Ortega-Sáenz, P., Molina, A., Franco-Obregón, A., Ureña, J. & Castellano, A. (1997) *Kidney Int.* **51,** 454–461.
29. Fearon, I. M., Palmer, A. C. V., Balmforth, A. J., Ball, S. G., Mikala, G., Schwartz, A. & Peers, C. (1997) *J. Physiol. (London)* **500,** 551–556.